Individual Cr atom in a semiconductor quantum dot: Optical addressability and spin-strain coupling

doi: 10.1103/PhysRevB.93.161301

PHYSICAL REVIEW B **93**, 161301(R) (2016)

Individual Cr atom in a semiconductor quantum dot: Optical addressability and spin-strain coupling

A. Lafuente-Sampietro,[1,2,3] H. Utsumi,[3] H. Boukari,[1,2] S. Kuroda,[3] and L. Besombes[1,2,*]

[1]*Université Grenoble Alpes, Institut Néel, F-38000 Grenoble, France*

[2]*CNRS, Institut Néel, F-38000 Grenoble, France*

[3]*Institute of Material Science, University of Tsukuba, Japan*

(Received 26 January 2016; revised manuscript received 31 March 2016; published 14 April 2016)

We demonstrate the optical addressability of the spin of an individual chromium atom (Cr) embedded in a semiconductor quantum dot. The emission of Cr-doped quantum dots and their evolution in magnetic field reveal a large magnetic anisotropy of the Cr spin induced by local strain. This results in the zero field splitting of the 0, ±1, and ±2 Cr spin states and in a thermalization on the magnetic ground states 0 and ±1. The observed strong spin to strain coupling of Cr is of particular interest for the development of hybrid spin-mechanical devices where coherent mechanical driving of an individual spin in an oscillator is needed. The magneto-optical properties of Cr-doped quantum dots are modeled by a spin Hamiltonian including the sensitivity of the Cr spin to the strain and the influence of the quantum dot symmetry on the carrier-Cr spin coupling.

DOI: 10.1103/PhysRevB.93.161301

In the last years, the development of semiconductor based nanoelectronics has driven intensive studies of individual spin dynamics and control in nanostructures. It has been shown that the electrical and the optical properties of a semiconductor quantum dot (QD) can be used to control the spin of individual carriers [1,2], ensemble of nuclei [3] as well as individual [4–7] or pairs [8,9] of magnetic atoms. In contrast to NV centers in diamond or molecular magnets, semiconductor QDs containing individual spins, and in particular a localized spin on a single atom, may be incorporated in conventional semiconductor devices [10] to add new quantum functionalities.

Among the variety of magnetic transition elements that can be incorporated in semiconductors, chromium (Cr) is of particular interest. Cr is incorporated in II-VI semiconductors as Cr^{2+} ions [11] (electronic configuration [Ar] $3d^4 4s^0 4p^0$) carrying a localized electronic spin $S = 2$ and an orbital momentum $L = 2$. Moreover, 90% of Cr isotopes have no nuclear spin limiting the number of spin states to five. The nonzero orbital momentum of Cr and spin-orbit coupling result in a large sensitivity of its spin to local strain. For such magnetic atom, static strain could be used to control the magnetic anisotropy and thus influence its spin memory [12,13]. This large spin to strain coupling also makes Cr a very promising spin *qubit* for the realization of hybrid spin-mechanical systems in which the motion of a microscopic mechanical oscillator would be coherently coupled to the spin state of a single atom [14,15].

We demonstrate here for the first time that the spin of an individual Cr atom can be detected optically. We show that the spin states of a Cr embedded in a CdTe/ZnTe QD, are split by a large magnetic anisotropy induced by biaxial strain in the plane of the QDs. At low temperature ($T = 5$ K), only the low energy states corresponding to the Cr spin $S_z = 0$ and $S_z = \pm1$ are detected by photoluminescence (PL). In some of the QDs, a significant mixing between dark and bright excitons attributed to the reduced symmetry of the dots is observed. The magnetic field dependence of the PL of an exciton in the exchange field of a Cr spin is analyzed. Magneto-optical properties of Cr-doped QDs can be modeled by a spin Hamiltonian including the strain induced fine structure of the magnetic atom, the exchange coupling with the carriers and the influence of the reduced symmetry of the QDs on the electron-hole exchange interaction and on the valence band.

Cr atoms are randomly introduced in CdTe/ZnTe self-assembled QDs grown by molecular beam epitaxy on ZnTe (001) substrates following the procedure described in Ref. [16]. The amount of Cr is adjusted to optimize the probability to detect QDs containing 1 or a few Cr atoms. The emission of individual QDs, induced by optical excitation with a dye laser tuned on resonance with an excited state of the dots [17], is studied in magnetic fields (up to 11 T) by optical micro-spectroscopy in Faraday configuration.

The low-temperature ($T = 5$ K) PL of the neutral exciton (X-Cr), positively charged (X^+-Cr) and negatively charged (X^--Cr) excitons and biexciton (X^2-Cr) of an individual Cr-doped QD (QD1) are reported in Fig. 1(a). Three emission lines are observed for the neutral species (X and X^2) and the positively charged excitons. The relative intensities of the lines and their splitting change from dot to dot as illustrated in Figs. 1(b) and 1(d). For some of the dots, a splitting of the central line is observed for X-Cr and X^2-Cr and an additional line appears on the low-energy side of the X-Cr spectra [see QD3 and QD4 Fig. 1(c) and 1(d)]. All these features result from the exchange coupling of the electron and hole spins with a single Cr spin.

In a II-VI semiconductor, the orbital momentum of the Cr connects the spin of the atom to its local strain environment through the modification of the crystal field and the spin-orbit coupling. For biaxial strain in the (001) plane, the ground state of a Cr spin is split by a strain induced magnetic anisotropy term $\mathcal{H}_{Cr,\varepsilon_\parallel} = D_0 S_z^2$ [18]. It was deduced from electron paramagnetic resonance of bulk Cr-doped CdTe that D_0 is positive for compressive biaxial strain [11]. In a self-assembled CdTe/ZnTe QD with large in-plane strain, the Cr spin energy levels are split with $S_z = 0$ at low energy [scheme in Fig. 1(a)].

*lucien.besombes@grenoble.cnrs.fr

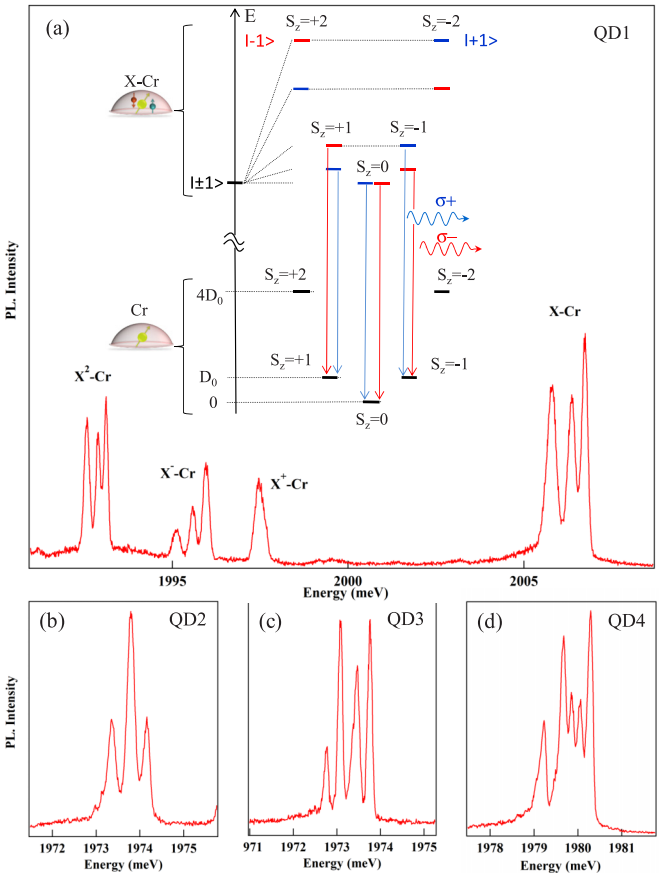

FIG. 1. (a) Low temperature ($T = 5$ K) PL of a QD (QD1) doped with a single Cr atom showing the emission from the neutral exciton (X-Cr), positively and negatively charged excitons (X^+-Cr and X^--Cr) and biexciton (X^2-Cr). The energy levels of the ground state (Cr), the bright exciton states ($|\pm 1\rangle$) coupled to the spin of a Cr (X-Cr), and dominant PL transitions ($\sigma+$, $\sigma-$) are illustrated in the inset. (b)–(d) PL of X-Cr in three other QDs (QD2, QD3, and QD4).

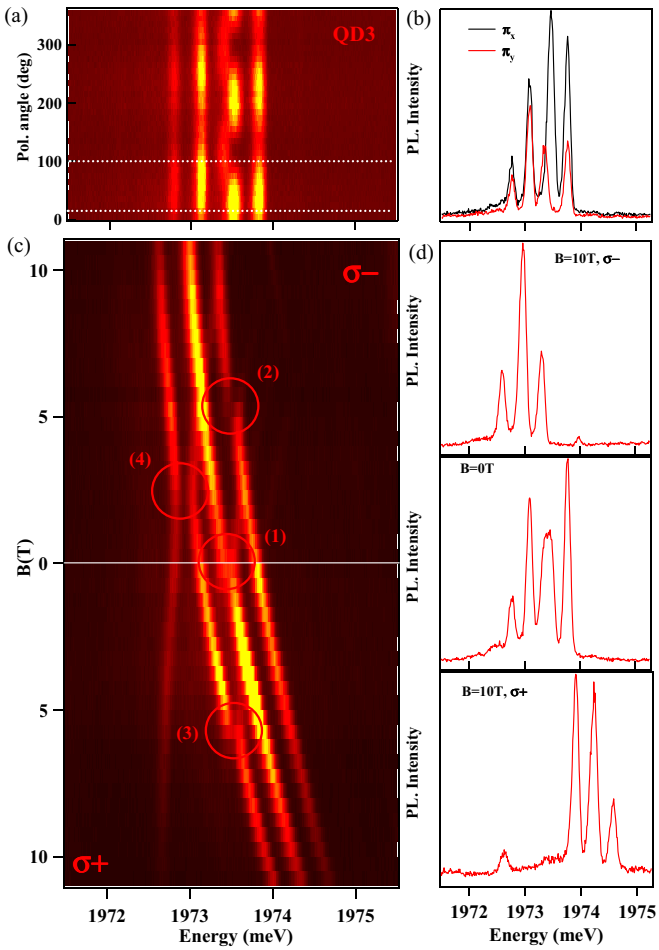

FIG. 2. (a) Linear polarization PL intensity map of X-Cr in QD3. (b) Corresponding linearly polarized PL spectra. (c) PL intensity map of X-Cr in QD3 vs magnetic field (B_z). (d) Corresponding circularly polarized PL spectra recorded at $B_z = 0$ and 10 T.

A value of D_0 in the 1-meV range can be expected for a CdTe layer strained on a ZnTe substrate [11,18].

When an electron-hole (e-h) pair is injected in a Cr-doped QD, the bright excitons are split by the exchange interaction between the spins of Cr and carriers. In flat self-assembled QDs, the heavy-holes and light-holes are separated in energy by the biaxial strain and the confinement. In a first approximation, the ground state in such QD is a pure heavy-hole ($J_z = \pm 3/2$) exciton and the exchange interaction with the Cr spin S is described by the spin Hamiltonian $\mathcal{H}_{c-\mathrm{Cr}} = I_{e\mathrm{Cr}}\vec{S}\cdot\vec{\sigma} + I_{h\mathrm{Cr}}S_zJ_z$, with $\vec{\sigma}$ the electron spin and J_z the hole spin operator. $I_{e\mathrm{Cr}}$ and $I_{h\mathrm{Cr}}$ are, respectively, the exchange integrals of the electron and the hole spins with the Cr spin. These exchange energies depend on the exchange constant of the $3d$ electrons of the Cr with the carriers in CdTe and on the overlap of the Cr atom with the confined carriers. The exchange interaction of the Cr spin is ferromagnetic for both electron and hole spins in common II-VI semiconductors and a typical exchange constant 4 to 5 times larger for the holes than for the electrons is also expected in CdTe [19,20].

For highly strained CdTe/ZnTe QDs with a weak hole confinement, the strain induced energy splitting of the Cr spin $D_0S_z^2$ is much larger than the exchange energy with the confined carriers ($D_0 \gg |I_{hCr}| > |I_{eCr}|$). The exchange interaction with the exciton acts as an effective magnetic field which further splits the Cr spins states $S_z = \pm 1$ and ± 2. The resulting X-Cr energy levels are presented in Fig. 1(a). The exciton recombination does not affect the Cr atom and its spin is conserved during the optical transitions. Consequently, the large strained induced splitting of the Cr spin is not directly observed in the optical spectra. However, at low temperature, the Cr spin thermalize on the low energy states $S_z = 0$ and ± 1. This leads to a PL dominated by three contributions: a central line corresponding to $S_z = 0$ and the two outer lines associated with $S_z = \pm 1$ split by the exchange interaction with the carriers.

The structure of the energy levels in Cr-doped QDs is confirmed by the evolution of the PL spectra in magnetic field. The circularly polarized PL of QD3 under a magnetic field applied along the QD growth axis is presented in Fig. 2 together with an analysis of the linear polarization at zero field. The central line ($S_z = 0$) is split and linearly polarized along two orthogonal directions [Figs. 2(a) and 2(b)]. As in nonmagnetic QD, this results from a coupling of the two bright

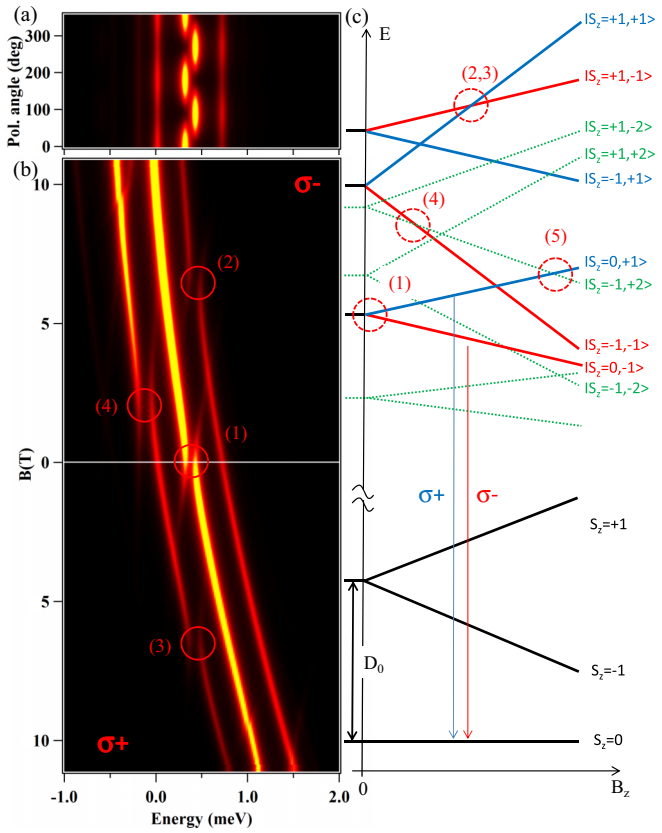

FIG. 3. (a) Calculated linear polarization PL intensity map of X-Cr at zero field and (b) calculated circularly polarized magnetic field dependence. Details of the model and parameters are listed in table II of the Supplemental Material. (c) Scheme of the magnetic field dependence of the energy levels of the low energy Cr spin states $S_z = 0$ and ± 1 and corresponding bright ($|+1\rangle$ blue, $|-1\rangle$ red) and dark ($|\pm 2\rangle$ green) X-Cr energy levels.

excitons $|\pm 1\rangle$ by (i) the short range e-h exchange interaction in the presence of valence band mixing and/or (ii) the long-range e-h exchange interaction in a QD with an in-plane shape anisotropy. This anisotropic e-h exchange energy mixes the bright exciton associated with the same Cr spin state, inducing an extra splitting between them. The mixing is maximum for the central pair of bright exciton ($S_z = 0$), which are initially degenerated. The outer lines are also slightly linearly polarized but the influence of the e-h exchange interaction is attenuated by the initial splitting of the $|\pm 1\rangle$ excitons induced by the exchange interaction with the Cr spin $S_z = \pm 1$. As illustrated in Fig. 3(c), the Zeeman energy of the exciton under magnetic field can compensate the exciton splitting induced by the exchange interaction with the Cr [21]. For QD3, this results in an anticrossing of $|+1\rangle$ and $|-1\rangle$ excitons due to the e-h exchange interaction around $B_z = 6$ T observed both in $\sigma+$ and $\sigma-$ polarizations [anticrossing (2) and (3) in Fig. 2(c)].

In some of the Cr-doped QDs, an additional line appears on the low-energy side of the PL spectra at zero magnetic field (line at 1972.7 meV for QD3 and at 1979.1 meV for QD4 in Fig. 1). An anticrossing of this line with the bright excitons is observed under B_z in $\sigma-$ polarization [anticrossing (4) in Fig. 2]. As illustrated in Fig. 3(c) this anticrossing arises from a mixing of the bright and dark excitons interacting with the same Cr spin state. Observed in $\sigma-$ polarization, it corresponds to the mixing of the exciton states $|-1\rangle$ and $|+2\rangle$ coupled to the Cr spin $S_z = -1$. This dark/bright exciton coupling δ_{12} is induced by the e-h exchange interaction in a confining potential of reduced symmetry (lower than C_{2v}) [22]. In such symmetry, the dark excitons acquire an in-plane dipole moment, which lead to possible optical recombination at zero magnetic field [23] as observed in QD3 and QD4. The oscillator strength of this "dark exciton" increases as the initial splitting between $|-1\rangle$ and $|+2\rangle$ excitons is reduced by the magnetic field [Fig. 3(c)].

We calculated the magneto-optic behavior of Cr-doped QDs like QD3 by diagonalizing the complete Hamiltonian of the e-h-Cr system [18]. We considered the general case of QDs with a symmetry lower than C_{2v} (truncated ellipsoidal lens for instance [22]), and took into account the influence of this reduced symmetry on the valence band and on the e-h exchange interaction. The population of the X-Cr spin states split by the large magnetic anisotropy and the carriers-Cr exchange interaction is described by a spin effective temperature T_{eff}. The results of the model obtained with $T_{\text{eff}} = 25$ K, $D_0 = 2.5$ meV and an electron-Cr (hole-Cr) exchange interaction $I_{e\text{Cr}} = -70$ μeV ($I_{h\text{Cr}} = -280$ μeV) are reported in Fig. 3 (parameters not specific to Cr-doped QDs are listed in Table II of Ref. [18]). The PL of X-Cr at zero field and its evolution in magnetic field can be qualitatively reproduced. In particular, the description of the spin states occupation by T_{eff} is sufficient to reproduce the observed emission from the three low energy X-Cr levels (Cr spin states $S_z = 0$ and ± 1). The splitting of the central line at zero field [anticrossing (1)] and the anticrossings under magnetic field [anticrossings (2) and (3) around $B_z = 6$ T for the Cr spin states $S_z = +1$ and anticrossings (4) with the dark exciton around $B_z = 2$ T] are also well reproduced by the model.

The magnetic anisotropy D_0 cannot be precisely extracted from the PL spectra. However, a too large value would produce a smaller PL intensity of the sates $S_z = \pm 1$ than observed experimentally. In addition, for $D_0 < 2.25$ meV, an anticrossing due to an electron-Cr flip-flop controlled by $I_{e\text{Cr}}$, labeled (5) in Fig. 3(c), would appear below $B_z = 11$ T on the central line in $\sigma+$ polarization.

To illustrate the influence of the QD symmetry on the magneto-optical properties of X-Cr, we compare in Fig. 4 the emission of a QD with cylindrical symmetry [QD2, Fig. 4(a)] and a QD with low symmetry [QD4, Fig. 4(c)]. For QD2, only three unpolarized lines are observed at zero field. Under magnetic field, each line is split and their energy follow the Zeeman and diamagnetic shift of the exciton. In QDs with a reduced symmetry such as QD4, a large contribution from the dark exciton is observed in the PL at zero field and the emission presents linearly polarized components. The characteristic bright exciton mixing induced by the e-h exchange interaction is observed in both circular polarization under magnetic field.

Investigating both the biexciton and the exciton in the same Cr-doped QD, we can also analyze the impact of the carrier-Cr interaction on the fine structure of the Cr spin. The magnetic field dependence of X^2-Cr and X-Cr emissions in QD4 are presented as a contour plot in Figs. 4(b) and 4(c), respectively. The PL under magnetic field of X-Cr and X^2-Cr present a

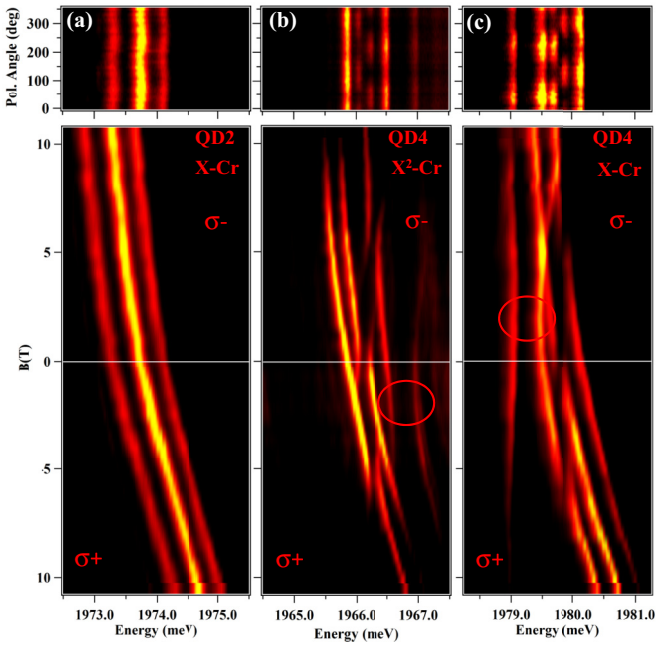

FIG. 4. Linear polarization intensity map (top) and intensity map of the longitudinal magnetic field dependence of the emission (bottom) of (a) X-Cr in QD2, (b) X^2-Cr in QD4, and (c) X-Cr in QD4.

mirror symmetry. In particular, the dark/bright exciton mixing observed around $B_z = 2.5$ T on the low-energy side of the PL in $\sigma-$ polarization for X-Cr is observed on the high energy side in $\sigma+$ polarization for X^2-Cr [circles in Figs. 4(b) and 4(c)].

If one considers the ground state of X^2 as a spin-singlet (total spin 0), it cannot be split by the magnetic field or the spin interaction part of the carriers-Cr Hamiltonian. The creation of two excitons in the QD cancels the exchange interaction with the Cr atom. Thus the PL of X^2-Cr is controlled by the final state of the optical transitions, i.e., the eigenstates of X-Cr, resulting in the observed mirror symmetry in the PL spectra. However, in some of the QDs, the X^2-Cr emission slightly deviates from this simple picture: a smaller energy splitting is observed for X^2-Cr compared to X-Cr (see X-Cr and X^2-Cr in QD1 and Ref. [18]). This shows that there is an interaction of X^2 with the Cr atom. It could result from a perturbation of the carriers' wave function by the interaction with the magnetic atom [24,25] or a modification of the local electric field which controls the Cr fine structure. Further investigations are required to explain this effect that goes beyond the purpose of this article.

To conclude, we demonstrated that the spin of a Cr atom in a semiconductor can be probed optically. The fine structure of the Cr is dominated by a magnetic anisotropy induced by strain in the plane of the QDs. The large spin to strain coupling of Cr, two orders of magnitude larger than for magnetic elements without orbital momentum (NV centers in diamond [26], Mn atoms in II-VI semiconductors [27]) suggests some possible development of coherent mechanical spin-driving of an individual magnetic atom in a nanomechanical oscillator. This single-spin system should allow, at low temperature, to enter some coupling regimes dominated by quantum coherent dynamics not reached until now in hybrid spin-mechanical devices.

The authors acknowledge financial support from the Labex LANEF for the Grenoble-Tsukuba collaboration. This work was realized in the framework of the Commissariat á l'Energie Atomique et aux Energies Alternatives (Institut Nanosciences et Cryogénie) / Centre National de la Recherche Scientifique (Institut Néel) joint research team NanoPhysique et SemiConducteurs.

[1] A. Greilich, D. R. Yakovlev, A. Shabaev, Al. L. Efros, I. A. Yugova, R. Oulton, V. Stavarache, D. Reuter, A. Wieck, and M. Bayer, Science **313**, 341 (2006).

[2] D. Press, T. D. Ladd, B. Zhang, and Y. Yamamoto, Nature (London) **456**, 218 (2008).

[3] B. Urbaszek, X. Marie, T. Amand, O. Krebs, P. Voisin, P. Maletinsky, A. Högele, and A. Imamoglu, Rev. Mod. Phys. **85**, 79 (2013).

[4] L. Besombes, Y. Leger, L. Maingault, D. Ferrand, H. Mariette, and J. Cibert, Phys. Rev. Lett. **93**, 207403 (2004).

[5] C. Le Gall, A. Brunetti, H. Boukari, and L. Besombes, Phys. Rev. Lett. **107**, 057401 (2011).

[6] A. Kudelski, A. Lemaitre, A. Miard, P. Voisin, T. C. M. Graham, R. J. Warburton, and O. Krebs, Phys. Rev. Lett. **99**, 247209 (2007).

[7] J. Kobak, T. Smoleński, M. Goryca, M. Papaj, K. Gietka, A. Bogucki, M. Koperski, J.-G. Rousset, J. Suffczyński, E. Janik, M. Nawrocki, A. Golnik, P. Kossacki, and W. Pacuski, Nat. Commun. **5**, 3191 (2014).

[8] L. Besombes, C. L. Cao, S. Jamet, H. Boukari, and J. Fernandez-Rossier, Phys. Rev. B **86**, 165306 (2012).

[9] O. Krebs and A. Lemaitre, Phys. Rev. Lett. **111**, 187401 (2013).

[10] M. Pierre, R. Wacquez, X. Jehl, M. Sanquer, M. Vinet, and O. Cueto, Nat. Nanotechnol. **5**, 133 (2010).

[11] J. T. Vallin and G. D. Watkins, Phys. Rev. B **9**, 2051 (1974).

[12] J. C. Oberg, M. Reyes Calvo, F. Delgado, M. Moro-Lagares, D. Serrate, D. Jacob, J. Fernandez-Rossier, and C. F. Hirjibehedin, Nat. Nanotechnol. **9**, 64 (2014).

[13] Yung-Chang Lin, Po-Yuan Teng, Po-Wen Chiu, and Kazu Suenaga, Phys. Rev. Lett. **115**, 206803 (2015).

[14] J. Teissier, A. Barfuss, P. Appel, E. Neu, and P. Maletinsky, Phys. Rev. Lett. **113**, 020503 (2014).

[15] P. Ovartchaiyapong, K. W. Lee, B. A. Myers, and A. C. Bleszynski Jayich, Nat. Commun. **5**, 4429 (2014).

[16] P. Wojnar, C. Bougerol, E. Bellet-Amalric, L. Besombes, H. Mariette, and H. Boukari, J. Cryst. Growth **335**, 28 (2011).

[17] L. Besombes and H. Boukari, Phys. Rev. B **89**, 085315 (2014).

[18] See Supplemental Material at http://link.aps.org/supplemental/10.1103/PhysRevB.93.161301 for further information about the fine structure of a Cr atom in a II-VI semiconductor

and the spin effective model of an exciton in a Cr-doped QD.

[19] W. Mac, A. Twardowski, and M. Demianiuk, Phys. Rev. B **54**, 5528 (1996).

[20] M. Herbich, W. Mac, A. Twardowski, K. Ando, Y. Shapira, and M. Demianiuk, Phys. Rev. B **58**, 1912 (1998).

[21] Y. Leger, L. Besombes, L. Maingault, D. Ferrand, and H. Mariette, Phys. Rev. Lett. **95**, 047403 (2005).

[22] M. Zielinski, Y. Don, and D. Gershoni, Phys. Rev. B **91**, 085403 (2015).

[23] M. Bayer, G. Ortner, O. Stern, A. Kuther, A. A. Gorbunov, A. Forchel, P. Hawrylak, S. Fafard, K. Hinzer, T. L. Reinecke, S. N. Walck, J. P. Reithmaier, F. Klopf, and F. Schafer, Phys. Rev. B **65**, 195315 (2002).

[24] L. Besombes, Y. Leger, L. Maingault, D. Ferrand, H. Mariette, and J. Cibert, Phys. Rev. B **71**, 161307(R) (2005).

[25] A. H. Trojnar, M. Korkusinski, U. C. Mendes, M. Goryca, M. Koperski, T. Smolenski, P. Kossacki, P. Wojnar, and P. Hawrylak, Phys. Rev. B **87**, 205311 (2013).

[26] A. Barfuss, J. Teissier, E. Neu, A. Nunnenkamp, and P. Maletinsky, Nat. Phys. **11**, 820 (2015)

[27] A. Lafuente-Sampietro, H. Boukari, and L. Besombes, Phys. Rev. B **92**, 081305(R) (2015)